Aroma synthesis and energy consumption in wine fermentation: a multiobjective optimization approach

Agustín G. Yabo, Céline Casenave

Aroma synthesis and energy consumption in wine fermentation: a multiobjective optimization approach ⋆

Agustín G. Yabo * **Céline Casenave** *

* *MISTEA, Université Montpellier, INRAE, Institut Agro, Montpellier, France (e-mail: agustin.yabo@inrae.fr, celine.casenave@inrae.fr).*

Abstract: Consumption of energy during wine fermentation process is directly linked to the temperature profile, which has also proven to have a major impact on the aromatic composition of the end product. This paper studies the impact of the temperature profile in wine fermentation, and the trade-off between the synthesis of aroma compounds and the energy required to regulate the temperature during the process. To this end, we consider a mathematical model representing the main chemical reactions of the wine fermentation including the synthesis of aromas, and a thermal model able to compute the energy required to follow the temperature profile in the fermenter. The objective is to maximize the aroma concentration in the final product while minimizing the energy required to refrigerate the fermenter. The compromise between the two optimization objectives forms Pareto-optimal front solutions, and different solutions are shown in order to better understand the impact of temperature on the process. The approach intends to highlight the potential of control theory techniques and optimization to tackle the inherent cost/quality trade-offs in wine fermentation process, towards a more sustainable energy-efficient winemaking industry.

Keywords: wine, aroma, wine fermentation, sustainable wine, temperature profile

1. INTRODUCTION

Wine industry is, as most of the sectors in agribusiness, a high energy-consuming industry, which therefore represents a non-negligible source of greenhouse gas emissions. The substantial growth in wine production has lately triggered numerous questions regarding the sustainability of the entire supply chain, from grape to glass (Bandinelli et al., 2020). Adopting sustainable practices in winemaking is not only favorable for the environment, but also for marketing. First of all, energy consumption has a direct impact on the final price of the product. Additionally, according to recent studies, wine consumers have become increasingly concerned by ethical and environmental issues, which can strongly influence purchase intentions in a competitive market (Forbes et al., 2009).

Behind the growing trend towards sustainable practices, there is always the need to preserve the quality of the end product. Aromas are among the most important factors that determine the character and quality of wines. So they must be taken into account along the transition towards sustainable winemaking. During fermentation, yeast convert the sugar available in the must in ethanol, CO_2, and a set of volatile compounds that compose the final flavour of the wine (Swiegers et al., 2005). While the complexity of the aromatic profile of wine has been proved to be impacted by many fermentation management practices, two factors have a particular importance: the nitrogen concentration in the must and the temperature profile during the fermentation process (Mouret et al., 2015).

Fermentation is an exothermic process, and thus the temperature in wine fermenters is always regulated by a refrigeration system. Cooling down the must during the fermentation process is highly energy-consuming, but it is essential to avoid yeast death, and the evaporation of volatile aroma compounds. On the other hand, at low temperatures yeast take longer to convert the available sugar, which leads to long and potentially more energy-consuming fermentations (Malherbe et al., 2004). The management of wine fermentation is thus a complex problem characterized by several trade-offs between the producer's objectives and constraints. In order to optimize this management and to propose adapted solutions, multi-objective optimization approaches and control theory must be used.

This is the objective of this paper, in which we consider the following multi-objective optimization problem: maximizing the liquid concentration of a given aroma compound at the end of the fermentation, while minimizing the total energy used by the cooling system. We focus on the production of a single aroma compound: IAA (isoamyl acetate) which is one of the main aroma compounds in wine fermentation, whose production is tightly linked to the temperature profile used in the fermentation.

To address the problem, we use a mathematical model representing oenological fermentation carried out by the *Saccharomyces cerevisiae* yeast strain. The model com-

⋆ This research project was funded by the French National Research Agency (ANR) under the grant agreement STARWINE (ANR-18-CE10-0013).

bines different works from the literature, that have been validated using experimental data. It accounts for the main chemical and physical reactions involved in wine fermentation: the main fermentation kinetics (Malherbe et al., 2004), the synthesis of IAA (Beaudeau et al., 2022b,a; Beaudeau, 2022), and the thermal dynamics throughout the fermentation process (Colombié et al., 2007). The thermal model represents heat transfer in the fermenter, by taking into account the heat generated by the bioprocess, as well as the refrigeration losses to the environment caused by evaporation and heat convection through the fermenter walls. Thus, the model is able to predict the energy required to regulate the temperature around a predefined profile.

The problem is first adressed by numerical exploration of the model. The final aroma concentration and the energy consumption were calculated using the model for a set of randomly generated temperature profiles. This provides a first insight into the more complex multi-objective dynamical optimization problem. As expected, the solutions complying with both optimization objectives form a Pareto-optimal front depending on the weight of each individual objective. Then, to further understand the dynamics of each solution, we solve the optimization problem for 3 sets of weight values. We thus obtained 3 different temperature profiles along the Pareto front that highlight different possible management strategies. Finally, we show a simulation of the chemical variables and the energy balance for one of these profiles in order to highlight the dynamics of the process.

To our understanding, literature is very scarce in this domain of research (Sablayrolles, 2009). Wine fermentation has been studied from a control-theory point of view in Martınez et al. (1999); Merger et al. (2017); Schenk et al. (2017), but none of the approaches model the presence of aromas in the must, which is key in representing the quality of the final product. In this context, our work is a proof of concept: while modeling a single ester does not capture the complexity of the aromatic profile of each wine, it is a first step towards a more comprehensive multi-objective control theory approach.

The paper is organized as follows: in Section 2, the model used to address the optimization problem is described. In Section 3, the optimization objectives are introduced, as well as the conditions and constraints of the implementation. In Section 4, the results of the multiobjective optimization problem are shown and interpreted. Finally, in Section 5, a brief discussion of the results and future works is provided.

2. MATHEMATICAL MODEL

2.1 Main fermentation kinetics

The first part of the model consists in the representation of the main fermentation kinetics which include the growth of the yeast on the nitrogen, and the conversion by the yeast of the sugar into ethanol and CO_2. The model equations are the one proposed in (Malherbe et al., 2004; Beaudeau et al., 2022b,a), that is:

- for the extracellular quantities, expressed in [g L^{-1}] with respect to the must volume inside the fermenter:

$$\begin{aligned}
\dot{S} &= -X\,\nu_{st}(S,E,N_{st},T),\\
\dot{CO_2} &= -\frac{1}{2.17}\dot{S},\\
\dot{E} &= -\frac{1}{2.17}\dot{S},\\
\dot{N} &= -\nu_N(N,E,A,T)X,\\
\dot{X} &= \mu(N_{in},E,A,T)X,
\end{aligned}$$

  where S is the glucose concentration, CO_2 represents the amount of $\mathrm{CO_2}$ released by the fermentation process, E is the concentration of ethanol, N is the concentration of assimilable nitrogen and X [10^9 cells L^{-1}] is the cell population of the yeast.
- for the intracellular quantities, expressed in [g 10^{-9}]:

$$\begin{aligned}
\dot{N_{in}} &= \nu_N(N,E,A,T) - \frac{1}{Y_{N_{st}}}\nu_{\mathrm{tr}}(N_{in},N_{st},T)\\
&\quad - (N_{in}+\alpha_1)\,\mu(N_{in},E,A,T),\\
\dot{N_{st}} &= \nu_{\mathrm{tr}}(N_{in},N_{st},T) - N_{st}\,\mu(N_{in},E,A,T),
\end{aligned}$$

  where N_{in} is the concentration of intracellular nitrogen and N_{st} represents the number of glucose transporters in a yeast cell. Both the nitrogen absorption rate and the growth rate are increasing with respect to $A \in [0, A^*]$, a dimensionless variable that accounts for cellular activity, that follows the dynamical equation

$$\dot{A} = \mu(N_{in},E,A,T)\,(A^* - A) - \kappa(T)A.$$

2.2 Temperature-dependent reaction rates

The ethanol-inhibited glucose transport rate responsible for sugar consumption and production of $\mathrm{CO_2}$ and ethanol, is defined as in (Malherbe et al., 2004; Beaudeau et al., 2022a) by:

$$\nu_{st}(S,E,N_{st},T) \doteq k_2(T)N_{st}\frac{S}{K_S + S(1+K_{Si}E^{\alpha_S})},$$

where the presence of N_{st} represents the catalyzing effect of glucose transporters over the conversion of sugar. The sugar transporter synthesis rate is defined as

$$\begin{aligned}
\nu_{\mathrm{tr}}(N_{in},N_{st},T) \doteq k_{N_{st}}(T)&\left(1-\frac{Q_0}{N_{in}}\right)^+\\
&- k_{d,N_{st}}\left(\frac{N_{st}}{k_{N_{st}}+N_{st}}\right),
\end{aligned}$$

composed of two terms for transporter synthesis and degradation, respectively. The operator f^+ accounts for the positive part of f, such that $f^+(x) = \max(f(x),0)$. The ethanol-inhibited nitrogen assimilation rate is

$$\nu_N(N,E,T) \doteq k_3(T)\frac{N}{K_N + N(1+K_{Ni}E^{\alpha_N})}.$$

Finally, the yeast growth rate, also inhibited by the presence of ethanol and proportional to the cellular activity, is defined as

$$\mu(N_{in},E,A,T) \doteq k_1(T)\left(1-\frac{N_{in,0}}{N_{in}}\right)^+\left(1-\frac{E}{E_{\max}}\right)^+ A.$$

All of the reaction rates are increasing with respect to the temperature, which is reflected on the parameters k_1, k_2, k_3, κ and $k_{N_{st}}$—that determine the maximal rate for each reaction—as

$$k_1(T) = a_1 T + b_1,$$
$$k_2(T) = a_2 T^2 - b_2 T + c_2,$$
$$k_3(T) = a_3 T^2 - b_3 T + c_3,$$
$$\kappa(T) = a_4 T - b_4,$$
$$k_{N_{st}}(T) = a_5 T^2 - b_5 T + c_2,$$

where the values of the parameters a_i, b_i and c_i correspond to those calibrated in Beaudeau et al. (2022a).

2.3 Energetic model

The heat transfer model is based on Colombié et al. (2007), and was validated against experimental wine fermentation data. The equation for energy conservation in the bioreactor involves the power accumulated by the must $P_a(CO_2, T, \dot{T})$, the power generated by the fermentation process $P_f(\dot{CO_2})$, the power exchanged by the walls of the fermenter $P_w(T - T_e)$ (where T_e is the room temperature), the dissipated power by evaporation of water and ethanol $P_e(CO_2, \dot{CO_2}, T)$, and the power used by the refrigeration system to cool down the bioreactor $Q_c(t)$. These expressions, all defined in kcal h^{-1}, depend on structural parameters (e.g. the dimensions and thermal conductivity of the fermentation tank, heat transfer coefficients, air temperature of the room, etc.) and were fixed in the present paper according to the cited work. $P_a(CO_2, T, \dot{T})$ is linear in $\dot{T}$, and so it can be expressed as $P_a(CO_2, T, \dot{T}) = \tilde{P}_a(CO_2, T)\dot{T}$. The energy balance equation becomes

$$\begin{aligned} P_f(\dot{CO_2}) = {} & \tilde{P}_a(CO_2, T)\dot{T} + P_w(T - T_e) \\ & + P_e(CO_2, \dot{CO_2}, T) + Q_c. \end{aligned} \tag{1}$$

During fermentation, if the cooling system is not active, then $Q_c(t) = 0$ and the temperature of the must rises freely. The dynamics of the non-controlled temperature T_{nc} can then be deduced from (1) and is given by $\dot{T}_{\mathrm{nc}} = v_{T_{\mathrm{nc}}}(CO_2, \dot{CO_2}, T_{\mathrm{nc}})$, with

$$v_{T_{\mathrm{nc}}}(CO_2, \dot{CO_2}, T_{\mathrm{nc}}) = \frac{1}{\tilde{P}_a(CO_2, T_{\mathrm{nc}})} \times$$
$$\left(P_f(\dot{CO_2}) - P_w(T_{\mathrm{nc}} - T_e) - P_e(CO_2, \dot{CO_2}, T_{\mathrm{nc}}) \right).$$

If the cooling system is activated, then $Q_c(t) > 0$ and the dynamics of the must temperature is written:

$$\dot{T} = v_{T_{\mathrm{nc}}}(CO_2, \dot{CO_2}, T) - \frac{Q_c}{\tilde{P}_a(CO_2, T)}. \tag{2}$$

2.4 Aroma dynamics

Models for the production of aromas can be found in Morakul et al. (2011); Mouret et al. (2014, 2015); Beaudeau et al. (2022a). The rate of production of aromas has been proven to depend on the rate of sugar consumption, and so Morakul et al. (2011) represented both gas and liquid phases of the aroma production as functions of $\dot{S}$. Thus, the dynamics of the aroma become

$$\dot{IAA} = -e^{Y_{IAA}(T, N_0)} \dot{S},$$
$$\dot{IAA}_{liq} = \dot{IAA} - Q_{CO_2}(\dot{CO_2}, T)\, e^{k_{IAA}(E,T)} IAA_{liq},$$

where IAA and IAA_{liq} are the concentrations [mg L^{-1}] of total IAA and liquid IAA in the must, respectively. Functions Q_{CO_2}, k_{IAA} and Y_{IAA} are defined as in Beaudeau et al. (2022a); in particular, $Y_{IAA}(T, N_0)$ is given by:

$$\begin{aligned} Y_{IAA}(\cdot) = {} & - D_1 + 10^3 D_2 N_0 - D_3 T \\ & + 10^6 D_4 N_0^2 + D_5 T^2 + D_6 10^3 N_0 T \end{aligned}$$

where D_i are positive constants.

2.5 Mass balance

As it is classical in wine fermentation processes, $CO_2(0) = E(0) = 0$, which means that

$$CO_2 = E = (S(0) - S)/2.17$$

for the whole bioprocess. Additionally, the model exhibits a mass conservation involving the nitrogen (both extracellular and intracellular) and the sugar transporters:

Lemma 1. The quantity $N + N_x$ is constant, with

$$N_x \doteq \left(N_{in} + \alpha_1 + \frac{1}{Y_{N_{st}}} N_{st} \right) X.$$

This property is used in Section 4 to illustrate the conversion of nitrogen into intracellular components.

3. OPTIMIZATION PROBLEM

3.1 Problem formulation

As explained in Section 1, the optimization problem we consider in the present paper is composed of two competing objectives: the maximization of the liquid concentration of the IAA at the end of the fermentation, and the minimization of the total energy used by the cooling system. These two quantites can be expressed as follows:

Total energy

$$J_1 = Q_T = \int_0^{t_f} Q_c(t)\, dt$$

Final liquid concentration of IAA

$$J_2 = IAA_{liq}(t_f)$$

where the final fermentation time t_f is defined in paragraph 3.3. The combination of the two objectives yields the multi-objective minimization problem characterized by the cost function:

$$J(T_p) = c_1 Q_T - c_2 IAA_{liq}(t_f). \tag{3}$$

where T_p is the temperature profile.

3.2 Optimization constraints

As it is customary in industrial winemaking, the temperature regulation is done through a cooling system that is able to compensate for the heat generated by the fermentation process. The characteristics of the cooling system impose constraints on the temperature profiles that can be applied. The temperature is bounded to lower and upper thresholds, and the rate of change of temperature is also bounded by the rate of CO_2 production, which is a standard practice in temperature regulation during winemaking (Sablayrolles and Barre, 1993; Morakul et al., 2013). These constraints are expressed as: [1]

$$18°C \leq T_p \leq 28°C, \qquad \left|\frac{\mathrm{d}T_p}{\mathrm{d}CO_2}\right| \leq \Delta T_{\max}. \tag{4}$$

where $\Delta T_{\max}$ is here fixed to 0.4. Moreover, since it is not possible to heat the must, Q_c must remain positive which restricts again the choice of temperature profiles that can be applied. From (2), we can calculate the value of the power $Q_c(\cdot)$ necessary to regulate the must temperature around a given temperature profile T_p. We obtain the following equation:

$$Q_c(\cdot) = \left(v_{T_{\mathrm{nc}}}(CO_2, \dot{CO_2}, T_p) - \dot{T}_p\right)\tilde{P}_a(CO_2, T_p)$$

To guarantee the positivity of Q_c, the temperature profile must finally verify the following constraint:

$$\dot{T}_p \leqslant v_{T_{\mathrm{nc}}}(CO_2, \dot{CO_2}, T_p). \tag{5}$$

3.3 Initial and final conditions

We suppose the initial temperature of the must is free. Additionally, following the experimental values chosen in Beaudeau et al. (2022a), we fix the initial sugar concentration to:

$$S(0) = 200 \text{ g L}^{-1}. \tag{6}$$

The duration of a wine fermentation t_f is not fixed a priori, but given by the terminal condition

$$S(t_f) = 5 \text{ g L}^{-1},$$

and so the simulations performed are assumed to finish when the concentration of sugar is below this threshold. Two values of initial nitrogen concentration are considered in the simulations for comparison:

$$N(0) \in \{0.14, 0.21\} \text{ g L}^{-1}. \tag{7}$$

3.4 Temperature profile expression

In Section 4, numerical simulations and optimization are performed to identify the temperature profiles that lead to good compromise between final aroma concentration and energy consumption. This profile has to verify the constraints given in (4) and (5). To easily comply with these constraints, the temperature profile will be expressed under the following form:

$$\dot{T}_p = \begin{cases} c_T\,\dot{CO_2} & \text{if } c_T\,\dot{CO_2} \leqslant v_{T_{\mathrm{nc}}}(CO_2, \dot{CO_2}, T_p) \\ v_{T_{\mathrm{nc}}}(CO_2, \dot{CO_2}, T_p) & \text{otherwise} \end{cases}$$

with c_T being the temperature control subject to $|c_T(t)| \leq \Delta T_{\max}$.

4. NUMERICAL EXPERIMENTS

4.1 Numerical simulations

Figure 1 shows 2000 numerical simulations of the system in the plane (J_1, J_2) for the initial sugar and nitrogen concentrations specified in (6) and (7). Each trajectory of the model is obtained for a temperature profile generated by a random piecewise constant control function $c_T(t)$ satisfying the constraints (4) at each time instant, and

[1] Note that one can easily verify that $\dot{CO_2}$ cannot vanish in finite time.

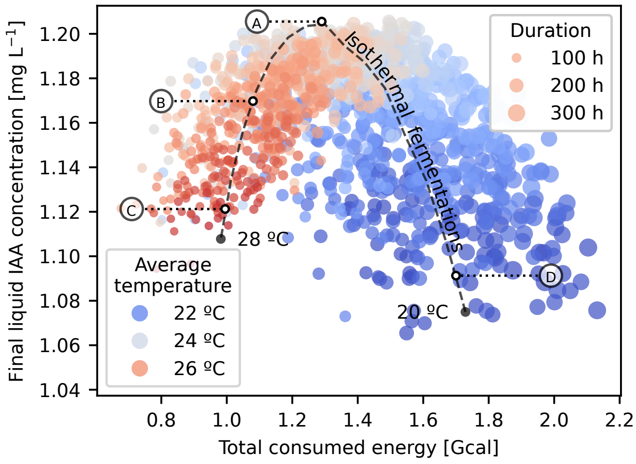

(a) $N(0) = 0.14$ g L^{-1}

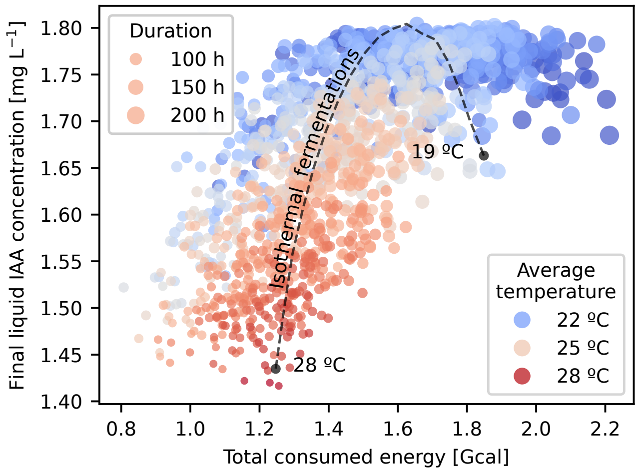

(b) $N(0) = 0.21$ g L^{-1}

Fig. 1. Final liquid IAA concentration J_2 and total consumed energy J_1 of 2000 fermentation simulations obtained with different random temperature profiles. Dot colors depend on the average must temperature of the fermentation, while the size is related to the fermentation duration. The dashed black line shows the pairs $(J_1 = Q_T, J_2 = IAA_{liq}(t_f))$ obtained from the isothermal fermentations (i.e. with $c_T = 0$ for all t) and for $T(0) \in [20, 28]$. In Subplot 1a, circles A, B, C and D denote the fermentations associated to the temperature profiles illustrated in Figure 2.

for a random initial temperature $T(0)$ within the temperature range (4). As expected due to the compromise between the two objectives J_1 and J_2, the random simulations produce Pareto-optimal fronts. The energy-efficient fermentations are characterized by a moderate to high average temperatures, and rather short durations, while the most energy-consuming fermentations occur for low temperatures, which consequently take longer to finish. The comparison between Subfigures 1a ($N(0) = 0.14$ g L^{-1}) and 1b ($N(0) = 0.21$ g L^{-1}) shows that the distribution of the (J_1, J_2) points can change depending on the value of $N(0)$. For the higher value of initial nitrogen ($N(0) = 0.21$ g L^{-1}), we observe higher values for both J_1 and J_2. However, the form of Pareto-optimal front is

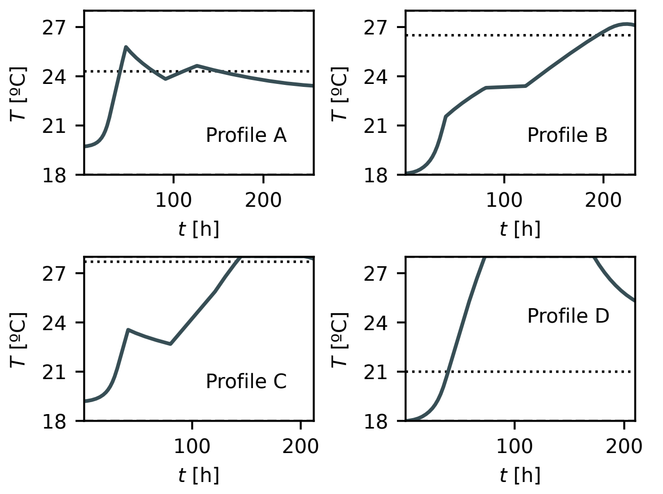

Fig. 2. Temperature profiles associated to the simulations denoted A, B, C and D in Figure 1a. The dotted black lines indicate the temperature of the isothermal fermentations producing the same final IAA_{liq}, and closest to each optimal solution in the (J_1, J_2) plane.

preserved, suggesting that the trade-off between the two objectives is inherent to the problem, independently of the initial nitrogen concentration.

4.2 Numerical optimization

In order to illustrate the optimal profile along the Pareto solutions, we solve the optimization problem given by the cost function (3) for different values of (c_1, c_2) through a SLSQP optimizer algorithm. To simplify the computations, the function c_T is parametrized in a 4-phase form:

$$c_T(t) = \begin{cases} k_a & if\ t < t_1, \\ k_b & if\ t_1 \leq t < t_2, \\ k_c & if\ t_2 \leq t < t_3, \\ k_d & if\ t \geq t_3, \end{cases}$$

for $t_1 < t_2 < t_3 < t_4$, and $|k_x| \leq \Delta T_{\max}$. As a result, 3 different profiles (A, B and C) are found, which are shown in Figures 2 and 1a. Additionally, a fourth profile D which is not a solution of the optimization problem is also plotted. We can observe that the profiles A, B and C have rather low initial temperatures, with initial free-heating phases (i.e. $Q_c(t) = 0$), followed by final control phases depending on each particular objective. When the priority is the synthesis of IAA (Profile A), the final temperature is intermediate, while when progressively assigning more weight to the energy factor (Profiles B and C), the final phases are characterized by higher temperatures—which are known to evaporate volatile aromas—and thus, shorter fermentations. Additionally, profiles A, B and C are able to produce the same amount of IAA than the isothermal fermentations denoted with a black dashed line, but with a considerable reduction in energy consumption (21%, 26% and 30%, respectively). Finally, Figure 3 shows a simulation of the model subject to the temperature profile B. The resulting CO_2 production rate dCO_2/dt exhibits a considerably smaller peak value than that of the isothermal analogous producing the same final liquid IAA concentration, which could explain the reduction in energy consumption. Indeed, the energy balance equation of Figure 4 shows how fermentation rate and energy consumption are tightly related, suggesting that an alternative approach could be to regulate directly the fermentation rate.

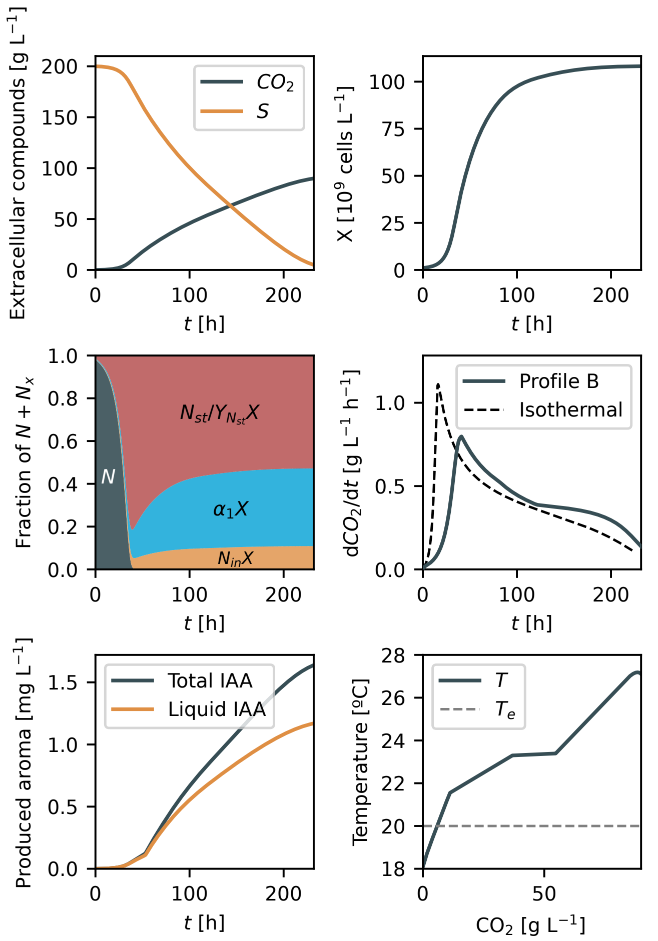

Fig. 3. Simulation of the main variables of the system for the temperature profile B. The transformation of N into α_1, N_{st} and N_{in} is illustrated using the fact that $N + N_x$ is constant. The reaction rate dCO_2/dt is shown for both Profile B and its isothermal analogous (at $T \approx 26.5$ ºC).

5. DISCUSSION AND CONCLUSION

In this paper, we performed an analysis of the impact of temperature regulation on aroma composition and energy consumption for energy-efficient winemaking. The study is based on a mathematical model representing oenological fermentation, synthesis of aromas and thermal dynamics, and the interplay between these three components. The objective is to maximize the aroma concentration in the final product while minimizing the energy required to refrigerate the fermenter, which produces a Pareto-optimal front on the plane of cost functions. Examples of temperature profiles along the Pareto solutions are illustrated, as well as a simulation of the optimized system. It is noteworthy that the obtained temperature profiles are not the unique solutions of the optimization problem. Indeed, multiple temperature profiles can yield the same pair (J_1, J_2), which indicates that further optimization criteria could be included in the analysis, such as additional aro-

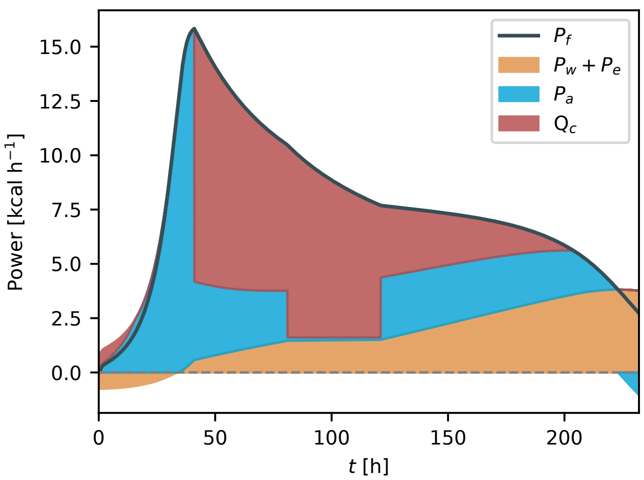

Fig. 4. Energy balance during the fermentation process, given by the equation $P_f = P_a + P_w + P_e + Q_c$. Negative quantities are shown below the x-axis. The total consumed energy corresponds to the area Q_c.

mas (e.g. isoamyl alcohol, isobutanol, ethyl hexanoate and ethyl octanoate, as modelled in Beaudeau et al. (2022a)). Multiple improvements to the approach are viable. An immediate next step will be to include nitrogen addition in the optimization approach, as it has been proven to have a major impact on the synthesis of aromas and on the duration of the bioprocess, for being the main limiting nutrient in oenological fermentation (Seguinot et al., 2018). Finally, a real-time feedback temperature regulation scheme will be developped based on online measurements of the concentration of aromas in the gas (and estimation of the liquid concentration). It will be implemented on the real process for experimental validation.

ACKNOWLEDGEMENTS

We thank Jean-Roch Mouret for the insight on the fermentation process, and Carine Bideaux for discussions on the dynamical model.

REFERENCES

Bandinelli, R., Acuti, D., Fani, V., Bindi, B., and Aiello, G. (2020). Environmental practices in the wine industry: an overview of the italian market. *British Food Journal*, 122(5), 1625–1646.

Beaudeau, F. (2022). *Modeling the synthesis of aroma during winemaking*. Ph.D. thesis, INSA Toulouse.

Beaudeau, F., Aceves Lara, C.A., and Bideaux, C. (2022a). Dynamic modelling of the effects of assimilable nitrogen addition on aroma synthesis during wine fermentation. Preprint.

Beaudeau, F., Aceves Lara, C.A., Godillot, J., Mouret, J.R., Trelea, I., and Bideaux, C. (2022b). Modeling the effects of assimilable nitrogen addition on fermentation in oenological conditions. Preprint.

Colombié, S., Malherbe, S., and Sablayrolles, J.M. (2007). Modeling of heat transfer in tanks during wine-making fermentation. *Food control*, 18(8), 953–960.

Forbes, S.L., Cohen, D.A., Cullen, R., Wratten, S.D., and Fountain, J. (2009). Consumer attitudes regarding environmentally sustainable wine: an exploratory study of the new zealand marketplace. *Journal of cleaner production*, 17(13), 1195–1199.

Malherbe, S., Fromion, V., Hilgert, N., and Sablayrolles, J.M. (2004). Modeling the effects of assimilable nitrogen and temperature on fermentation kinetics in enological conditions. *Biotechnology and bioengineering*, 86(3), 261–272.

Martınez, G., López, A., Esnoz, A., Vırseda, P., and Ibarrola, J. (1999). A new fuzzy control system for white wine fermentation. *Food Control*, 10(3), 175–180.

Merger, J., Borzi, A., and Herzog, R. (2017). Optimal control of a system of reaction–diffusion equations modeling the wine fermentation process. *Optimal Control Applications and Methods*, 38(1), 112–132.

Morakul, S., Mouret, J.R., Nicolle, P., Aguera, E., Sablayrolles, J.M., and Athès, V. (2013). A dynamic analysis of higher alcohol and ester release during winemaking fermentations. *Food and Bioprocess Technology*, 6(3), 818–827.

Morakul, S., Mouret, J.R., Nicolle, P., Trelea, I.C., Sablayrolles, J.M., and Athes, V. (2011). Modelling of the gas–liquid partitioning of aroma compounds during wine alcoholic fermentation and prediction of aroma losses. *Process Biochemistry*, 46(5), 1125–1131.

Mouret, J.R., Farines, V., Sablayrolles, J.M., and Trelea, I.C. (2015). Prediction of the production kinetics of the main fermentative aromas in winemaking fermentations. *Biochemical Engineering Journal*, 103, 211–218.

Mouret, J., Camarasa, C., Angenieux, M., Aguera, E., Perez, M., Farines, V., and Sablayrolles, J.M. (2014). Kinetic analysis and gas–liquid balances of the production of fermentative aromas during winemaking fermentations: effect of assimilable nitrogen and temperature. *Food research international*, 62, 1–10.

Sablayrolles, J.M. and Barre, P. (1993). Kinetics of alcoholic fermentation under anisothermal enological conditions. i. influence of temperature evolution on the instantaneous rate of fermentation. *American journal of enology and viticulture*, 44(2), 127–133.

Sablayrolles, J. (2009). Control of alcoholic fermentation in winemaking: Current situation and prospect. *Food research international*, 42(4), 418–424.

Schenk, C., Schulz, V., Rosch, A., and von Wallbrunn, C. (2017). Less cooling energy in wine fermentation–a case study in mathematical modeling, simulation and optimization. *Food and Bioproducts Processing*, 103, 131–138.

Seguinot, P., Rollero, S., Sanchez, I., Sablayrolles, J.M., Ortiz-Julien, A., Camarasa, C., and Mouret, J.R. (2018). Impact of the timing and the nature of nitrogen additions on the production kinetics of fermentative aromas by saccharomyces cerevisiae during winemaking fermentation in synthetic media. *Food microbiology*, 76, 29–39.

Swiegers, J., Bartowsky, E., Henschke, P., and Pretorius, I. (2005). Yeast and bacterial modulation of wine aroma and flavour. *Australian Journal of grape and wine research*, 11(2), 139–173.